Transformation of magnetic transfer functions in apparent resistivities and phases - the general case

M. Becken, Institut für Angewandte Geophysik, TU Berlin
L. B. Pedersen, Department of Geophysics, Uppsala University

Introduction

The method presented here is a direct transformation of magnetic transfer functions into apparent resistivities and phases. The derivation is an extension of the two-dimensional procedure developed by Gharibi and Pedersen [2000] to arbitrary conductivity structures in the subsurface.

The VLF technique (very-low-frequency) is a well established electromagnetic tool for mapping near surface structures of geological targets. Here, artificial source fields generated by powerful VLF transmitters situated at several locations all over the world and radio transmitters are used in induction studies for shallow applications. By combining two or more transmitters located in different directions, one can calculate a set of transmitter-independent induction parameters for each point of measurement (Pedersen [1989], Pedersen et al. [1994], Gharibi & Pedersen [2000]), which are the same as the magnetic transfer function in geomagnetic depth sounding applications (GDS). The Geological Survey of Sweden (SGU) operates a 'tensor'-VLF device as an add-on tool in airborne surveys and acquired maps of magnetic transfer functions (tipper) for frequencies around 16 kHz.

We show, that the magnetic transfer function is related to the full TE-mode impedance tensor besides a constant in the electric field, which has to be estimated by other means. Use must be made of the potential field character of the magnetic field in the air half-space, yielding an successive approximation of the anomalous magnetic fields for an arbitrary primary magnetic field. When the anomalous vertical component is explicitly known, solving Faraday's equation in the wavenumber domain by using the divergence theorem leads to an estimation of the anomalous electric field of TE-mode. The normal electric field is provided by an impedance measurement at one point in the area of investigation.

We demonstrate, that structural information in terms of apparent resistivity and phase reflecting different kinds of lithologies can be extracted from magnetic measurements and related to geological investigations. In the following sections, the decomposition of electric and magnetic fields and transfer functions is introduced and the procedure of the transformation is developed.

Theory

Basic Equations: We use a right-handed cartesian coordinates (x, y, z) with unit vectors $(\hat{x}, \hat{y}, \hat{z})$, where $\hat{z}$ is directed downward. The electric and magnetic fields are given with a time dependency $\left\{ \begin{matrix} \mathbf{E} \\ \mathbf{H} \end{matrix} \right\} \sim e^{i\omega t}$, where ω is the angular frequency. The magnetic permeability

is assumed to be the vacuum permeability μ_0 everywhere, which gives the choice of either working with the magnetic field or the magnetic flux density $\mathbf{B} = \mu_0\mathbf{H}$, since they are linked by a constant. The field relations in homogeneous regions of conductivity σ is described by Ampere's and Faraday's equation

$$\nabla \times \mathbf{H} = \mathbf{J} + \mathbf{J}^{ext} \ , \ \ \nabla \times \mathbf{E} = -i\omega\mathbf{B} \ , \tag{1}$$

where displacement currents have been neglected (quasi-static approximation). The electric field enters the first of equation (1) via Ohm's law, linking the internal currents as $\mathbf{J} = \sigma\mathbf{E}$. External currents $\mathbf{J}^{ext}$ cross the air-earth interface, if the source is galvanically coupled to the conductive region. The far fields of Radio- and VLF-transmitters can be considered as inductively coupled plane waves. Hence, all currents are induced and thus of internal origin and the source term in the first equation (1) is regarded as zero.

Since $\mathbf{B}$ is divergence-free everywhere, and in one-dimensional regions away from sources, $\mathbf{J}$ is divergence-free as well, both fields can be described by two scalar potentials φ_E, φ_M (Vasseur & Weidelt [1977]) as:

$$\mathbf{B} = \mathbf{B}_E + \mathbf{B}_M \ , \ \ \mathbf{J} = \mathbf{J}_E + \mathbf{J}_M \ . \tag{2}$$

where

$$\mathbf{B}_E = \nabla \times \nabla \times (\hat{z}\varphi_E) \ , \ \mathbf{B}_M = \nabla \times (\hat{z}\mu_0\sigma\varphi_M) \tag{3}$$

$$\mathbf{J}_E = -i\omega\nabla \times (\hat{z}\sigma\varphi_E) \ , \ \mathbf{J}_M = \nabla \times \nabla \times (\hat{z}\sigma\varphi_M) \tag{4}$$

Introducing the constitutive relations yields the corresponding equations for the magnetic field $\mathbf{H}$ and the electric field $\mathbf{E}$:

$$\mathbf{H}_E = \frac{1}{\mu_0}\nabla \times \nabla \times (\hat{z}\varphi_E) \ , \ \mathbf{H}_M = \nabla \times (\hat{z}\sigma\varphi_M) \tag{5}$$

$$\mathbf{E}_E = -i\omega\nabla \times (\hat{z}\varphi_E) \ , \ \mathbf{E}_M = \frac{1}{\sigma}\nabla \times \nabla \times (\hat{z}\sigma\varphi_M) \tag{6}$$

Note, that application of the curl operator to the vector $\hat{z}\varphi_{E,M}$, pointing in vertical direction, produces a horizontal vector. Therefore, the systems $\{\mathbf{J}_E, \mathbf{E}_E\}$ and $\{\mathbf{B}_M, \mathbf{H}_M\}$ have no vertical components and are tangential to the earth's surface. They are considered as tangential-electric and tangential-magnetic systems, respectively, or, say, TE-mode and TM-mode (Weidelt, Lecture notes).

The potentials are likewise chosen so that Maxwell's equations and the material equations hold true for each mode separately. Either modes may be considered independently in one-dimensional regions, although they are coupled in anomalous regions. Therefore we may write

$$\nabla \times \mathbf{H}_E = \sigma\mathbf{E}_E \ \ , \ \ \nabla \times \mathbf{H}_M = \sigma\mathbf{E}_M \tag{7}$$

$$\nabla \times \mathbf{E}_E = -i\omega\mathbf{B}_E \ \ , \ \ \nabla \times \mathbf{E}_M = i\omega\mathbf{B}_M \tag{8}$$

for Ampere's and Faraday's equation, respectively.

Consider now a *non-conductive region* like the region of measurement above the surface. From equations (2) - (6) immediately follows, that $\mathbf{J}_E, \mathbf{J}_M, \mathbf{B}_M$ and $\mathbf{H}_M$ vanish in free space. Thus, the magnetic field to be measured is entirely of TE-mode and furthermore entirely connected to the electric field of TE-mode. The TM-mode electric field in a non-conductive region is curl-free (compare equation (8)). Hence, it is a potential field in combination with its vanishing divergence, like the magnetic TE-mode field is Laplacian. Note, that solving Faraday's equation to estimate electric fields from surface magnetic measurements can only

TF	1-D case (normal structure)	2-D case (strike in x-dir.)	3-D case (general case)
$T_x =$	0	0	$f(\mathbf{r})$
$T_y =$	0	$f(y)$	$f(\mathbf{r})$
$Z_{E,xx} =$	0	0	$f(\mathbf{r})$
$Z_{E,xy} =$	$Z_{E,xy}^n = const$	$f(y)$	$f(\mathbf{r})$
$Z_{E,yx} =$	$Z_{E,xy}^n = -Z_{E,xy}^n$	$Z_{E,xy}^n$	$f(\mathbf{r})$
$Z_{E,yy} =$	0	0	$f(\mathbf{r})$
$Z_{M,xx} =$	0	0	$f(\mathbf{r})$
$Z_{M,xy} =$	0	0	$f(\mathbf{r})$
$Z_{M,yx} =$	0	$f(y)$	$f(\mathbf{r})$
$Z_{M,yy} =$	0	0	$f(\mathbf{r})$

Table 1: Magnetic and magnetotelluric transfer functions (TF) of tipper vector and impedance tensor of a conductive earth subject to a homogeneous TE-mode source field.

provide the TE-mode part of the electric field (besides a constant), which differs from the total electric field one would measure directly.

The VLF-fields are inductively coupled to the earth. The primary magnetic field is therefore of TE-mode. This states, that the TM-mode electric field at the earth's surface is entirely of internal origin. The measured quantities are finally given in their decomposed notation as:

$$\mathbf{B} = \mathbf{B}_E^n + \mathbf{B}_E^a \tag{9}$$

$$\mathbf{E} = \mathbf{E}_E^n + \mathbf{E}_E^a + \mathbf{E}_M^a \ . \tag{10}$$

Here, the superscripts n and a denote the normal fields in the *plane wave approximation* (of external and internal origin) and the anomalous fields (of internal origin), respectively. $\mathbf{B}_E^n$ and $\mathbf{E}_E^n$ are assumed to be independent of horizontal space coordinates and are estimated in normal regions.

The transfer functions, which are derived from measured magnetotelluric fields, may be decomposed like the fields themselves. The magnetic transfer functions is entirely of TE-mode, since the concerned fields are only of TE-mode. The tipper vector $\mathbf{T}_E$ is defined via the equation

$$B_{E,z} = \mathbf{T}_E \mathbf{B}_{E,h} \ . \tag{11}$$

Here, the subscript h denotes the horizontal vector.

The impedance tensor $\mathbf{Z} = \mathbf{Z}_E + \mathbf{Z}_M$ relates the horizontal magnetic field of TE-mode to the horizontal electric field of TE- and TM-mode as

$$\mathbf{E}_{E,h} + \mathbf{E}_{M,h} = (\mathbf{Z}_E + \mathbf{Z}_M)\,\mathbf{B}_{E,h} \tag{12}$$

Each element of the impedance tensor is decomposed into a transfer function of TE- and TM-mode, respectively. Note, that, according to the previous derivations, the full impedance tensor cannot be derived from the tipper components, since the tipper is of pure TE-mode, but the impedance is a mixture of both modes.

Some properties or those sets of transfer function related to the dimensionality of the earth are given in table 1. They are only valid for a plane wave primary field, as it can be assumed in the scope of the VLF method.

Estimation of the Electric TE-Mode Field: Magnetic tensor measurements are commonly presented as magnetic transfer functions. In order to derive the TE-mode electric field, magnetic field vectors must be extracted from the transfer functions. Then, from the vertical magnetic field, the horizontal electric field of TE-mode may be calculated and according to equation (12), the TE-mode impedance tensor will be estimated. The subsequent derivation of the tipper transformation is more convenient in wavenumber space.

The spatial Fourier transform of a function $f(\mathbf{r})$ is denoted by $\tilde{f}(\mathbf{k})$, where $\mathbf{r} = (x, y)^T$ is the horizontal space vector and $\mathbf{k} = (k_y, k_x)^T$ is the wavenumber vector. Then

$$\tilde{f}(\mathbf{k}) = \frac{1}{2\pi} \int_{-\infty}^{\infty} \int_{-\infty}^{\infty} f(\mathbf{r}) e^{-i\mathbf{k}\cdot\mathbf{r}} d\mathbf{r} \tag{13}$$

and the inverse Fourier transform is given by

$$f(\mathbf{r}) = \frac{1}{2\pi} \int_{\infty}^{-\infty} \int_{\infty}^{-\infty} \tilde{f}(\mathbf{k}) e^{i\mathbf{k}\cdot\mathbf{r}} d\mathbf{k} \ . \tag{14}$$

Derivative operators in space domain turn out as multiplication in wavenumber domain: $\partial/\partial x \left[f(\mathbf{r}) \right]$ transforms to $ik_x \tilde{f}(\mathbf{k})$ and $\partial/\partial y \left[f(\mathbf{r}) \right]$ to $ik_y \tilde{f}(\mathbf{k})$, respectively.

Since the magnetic field in the air is a potential field, knowledge of one of its components on a (closed) surface is sufficient to calculate the two remaining field components. Therefore, the solution of equation (11) for B_z is unique.

An iterative solution of the tipper decomposition is suggested similar to the one used by Gharibi & Pedersen [2000] in their two-dimensional tipper transformation. The mathematical treatment of the three-dimensional case is a simple expansion of the two-dimensional solution, but calculation of the Hilbert transformation is performed in wavenumber domain. Here, a drift in the data can easily be corrected for by taking all magnetic field components to be zero at zero wavenumber.

The Hilbert transformation of a potential vector field $\mathbf{V}(\mathbf{r}, z)$, which is known on a closed surface, is transformed to wavenumber domain (Pedersen [1989]) as

$$\tilde{V}_z(\mathbf{k}, 0) = -\frac{i\mathbf{k}}{k} \cdot \tilde{\mathbf{V}}_h(\mathbf{k}, 0) \ , \tag{15}$$

where k denotes the absolute value of the wavenumber vector. The reverse formulation of equation (15) is

$$\tilde{\mathbf{V}}_h(\mathbf{k}, 0) = \frac{i\mathbf{k}}{k} \tilde{V}_z(\mathbf{k}, 0) \ . \tag{16}$$

The latter relation will be utilized for extracting magnetic field vectors from known tipper vectors.

For a given normal magnetic field $\mathbf{B}_h^n$, a first approximation of the (anomalous) vertical field component can be estimated according to $B_z^0(\mathbf{r}, 0) = \mathbf{T}(\mathbf{r}, 0)\mathbf{B}_h^n$. Fourier transformation to wavenumber domain permits a first estimation of the anomalous horizontal field using equation (16). Adding the derived anomalous part to the normal field enables a new estimation of the vertical component. Hence, a number of iterations j are performed following the procedure

$$B_z^{j+1}(\mathbf{r}, 0) = \mathbf{T}(\mathbf{r}, 0)\mathbf{B}_h^j(\mathbf{r}, 0) \ , \tag{17}$$

$$\tilde{\mathbf{B}}_h^{a,j+1}(\mathbf{k}, 0) = \frac{i\mathbf{k}}{k} \tilde{B}_z^{j+1}(\mathbf{k}, 0) \ , \tag{18}$$

$$\mathbf{B}_h^{j+1}(\mathbf{r}, 0) = \mathbf{B}_h^{a,j+1}(\mathbf{r}, 0) + \mathbf{B}_h^n \ . \tag{19}$$

A criterion to stop the iterative process is required. Here, we use that the maximum difference of the vertical component between the present and the previous iteration $\left| B_z^j(\mathbf{r}_m, 0) - B_z^{j-1}(\mathbf{r}_m, 0) \right|$ at the point $(\mathbf{r}_m, 0)$ should be less than δB_z.

In order to describe the three-dimensionality of the problem, the same procedure must be repeated for another primary magnetic field, which is preferably perpendicular to the first one.

From the vertical magnetic field, the TE-mode electric field may be derived from Faraday's law: Taking $\mathbf{E}_E(\mathbf{r}, 0) = \mathbf{E}_E^n + \mathbf{E}_E^a(\mathbf{r}, 0)$, the anomalous electric field is given in wavenumber domain by

$$\hat{z} \times \widetilde{\mathbf{E}}_E^a(\mathbf{k}, 0) = \frac{\omega \mathbf{k}}{k^2} \widetilde{B}_z(\mathbf{k}, 0) \ , \tag{20}$$

where use was made of the vanishing horizontal divergence

$$i\mathbf{k} \cdot \widetilde{\mathbf{E}}_E^a(\mathbf{k}, 0) = 0 \ , \tag{21}$$

since the TE-mode electric field has no vertical component. Division by k^2 is required in equation (20), which causes a singularity at $k = 0$. Anyway, the Fourier coefficient at the singular point in wavenumber domain is equivalent to shifting the field in space domain of the amount of the medium anomalous field without affecting the change of the electric field. Therefore, we take $\widetilde{\mathbf{E}}_E^a(\mathbf{k} = 0, 0) \equiv 0$ for the moment.

Back-transformation to space domain yields the anomalous electric field besides an unknown shift $d\mathbf{E}_E$. The total electric field (of TE-mode) is than given by $\mathbf{E}_E(\mathbf{r}, 0) = \mathbf{E}_E^n + [\mathbf{E}_E^a(\mathbf{r}, 0) - d\mathbf{E}_E] + d\mathbf{E}_E$. Suppose now, that the impedance at one point is known, e.g. $Z_{ij}(\mathbf{r}_0, 0)$, and that this measurement has been carried out in a one-dimensional region, sufficiently far away from distortions. In this case, $\mathbf{E}_E^a(\mathbf{r}_0, 0) = 0$, the total electric field corresponds to the normal TE-mode electric field since there is no TM-mode excited in normal regions, and furthermore, there is no magnetic anomaly to be observed. Hence, the impedance is simplified to $Z_{ij}(\mathbf{r}_0, 0) = E_{i,E}^n / B_{j,E}^n$, from which the electric field can be calculated for any normal magnetic field. The previously estimated anomalous electric field $[\mathbf{E}_E^a(\mathbf{r}, 0) - d\mathbf{E}_E]$ may now be shifted to the desired level at the point $(\mathbf{r}_0, 0)$, which should result in the correct level for the whole surface, provided data were error free. Therefore, knowledge of $d\mathbf{E}_E$ is easily obtained. Since the measured tipper values are erroneous, one may expect a slight misfit of the calculated impedance function, of course, but as we shall see later, the method seems to work in a stable way and gives good structural resolution.

Having found horizontal electric and magnetic fields for two polarizations, the corresponding impedance tensor of TE-mode is estimated. A rotational invariant parameter is, however, more suitable for visualizing the results in terms or apparent resistivity and phases. For this purpose, the determinant of the impedance tensor is calculated according to

$$\|Z_E\|^2 = Z_{xx} Z_{yy} - Z_{xy} Z_{yx} \ , \tag{22}$$

which is related to apparent resistivity and phase as

$$\rho_E = \frac{\mu_0}{\omega} \|Z_E\|^2 \tag{23}$$

$$\phi_E = \arg\left\{\|Z_E\|\right\} \ . \tag{24}$$

Application to Airborne VLF-Data in SE-Sweden

The aim of the subsequent description of the application to field data is to demonstrate, that the suggested algorithm is stable, yields reasonable results, and facilitates interpretation of magnetic transfer functions.

The data shown here are collected and provided by the Geological Survey of Sweden (SGU) during airborne surveys in Sweden. They used the transmitters Rugby (United Kingdom) and Bordeaux (France) in order to estimate magnetic transfer functions for frequencies around

$16\,kHz$. The azimuthal angle differs only about 20 degrees. Fortunately, predominant strike-direction in the measurement area is east. Northward striking structures are worse resolved due to the choice of transmitters. Reference is made to Gharibi & Pedersen [1999], whose two-dimensional tipper transformation was applied to profiles in the same area.

For the purpose of the three-dimensional tipper transformation, the originally irregularly spaced data (flight line separation $\sim 200\,m$, lines in S-N direction, point distance on each line $\sim 15\,m - 20\,m$) were interpolated to a regular grid of $50\,m$ point to point distance in both northern and eastern directions. We have not performed a downward continuation of the fields from the measurement height ($\sim 70\,m$) to the surface.

Geological Background: The area investigated lies within the map (Stockholm 10 I SO, SGU), southeastern of Stockholm, and is part of the Bergslagen region, which has been a major metal producer for more than one millennium (Allen et al. [1996]). The Bergslagen area is the type location of the term "skarn" and several other mineral species. Banded iron formations and various types of skarn deposits build a diverse range of ore deposits. Most of them occur in metavolcanic rocks and associated facies.

The basement, nowadays covered to a great extent by quaternary sediments, is of early Proterozoic age and part of a felsic magmatic region of mainly medium to high metamorphic grade in the Baltic shield. Allen et al. [1996] interpreted the region as an extensional basin in the environment of an active continental margin, comprising several stages of pre- and post-tectonic magmatic intrusions through the evolution.

The metavolcanic and metasedimentary rocks shown in fig. 1a are deformed into steep doubly plunging, mainly east-west orientated synclines, partly wrapping around rheologically more competent granitoid and granodioritic intrusions. Thin-sheet like intrusions were involved in the folding and show up as macro folds of wavelengths of more than $30\,km$, embedded in deformed metasediments.

Since the competent rocks were very resistive against glacial erosion during the quaternary ice-sheet coverage of the Baltic Shield, they gently build up as topographic highs, whereas the valleys covered by thin electrical conductive quaternary alluvium, indicate underlaying rheologically weaker metavolcanics and -sediments.

Maps of Apparent Resistivities and Phases: As an example of the data set, the real part of T_x is shown in fig. 1b, mainly indicating east-west striking structures. The $15\,km \times 25\,km$ area is the same as shown in the geological map. Typical values of the tipper in this area range from -0.4 to 0.4. The plot is superimposed by the topography, which has been plotted as a gray shaded relief.

The required medium electric field over the whole area was estimated by assuming a half-space with a resistivity of $5000\,\Omega m$, overlain by a thin-sheet of $0.015\,S$. This corresponds to an apparent resistivity of around $3300\,\Omega m$. It was experienced, that this guess leads to reasonable results, but it should be taken into account that the range of apparent resistivities and phases is thereby determined. Hence, one should focus on the trend rather than the absolute values.

Fig. 2 shows the results of the tipper transformation in terms of apparent resistivity and phase of the determinant of the impedance tensor, superimposed by the topography. Gray to Black denotes high apparent resistivities and phases below 45 degrees, light colours indicate low apparent resistivities and high phases, respectively. White lines indicates the coast line and lakes.

Apparent resistivity and phase correlate significantly with lithological units as shown in the geological map. The apparent resistivity (fig. 2b) is low in sediment filled valleys, which were described previously, whereas the phase (fig. 2a) is higher than 45 degrees in these regions,
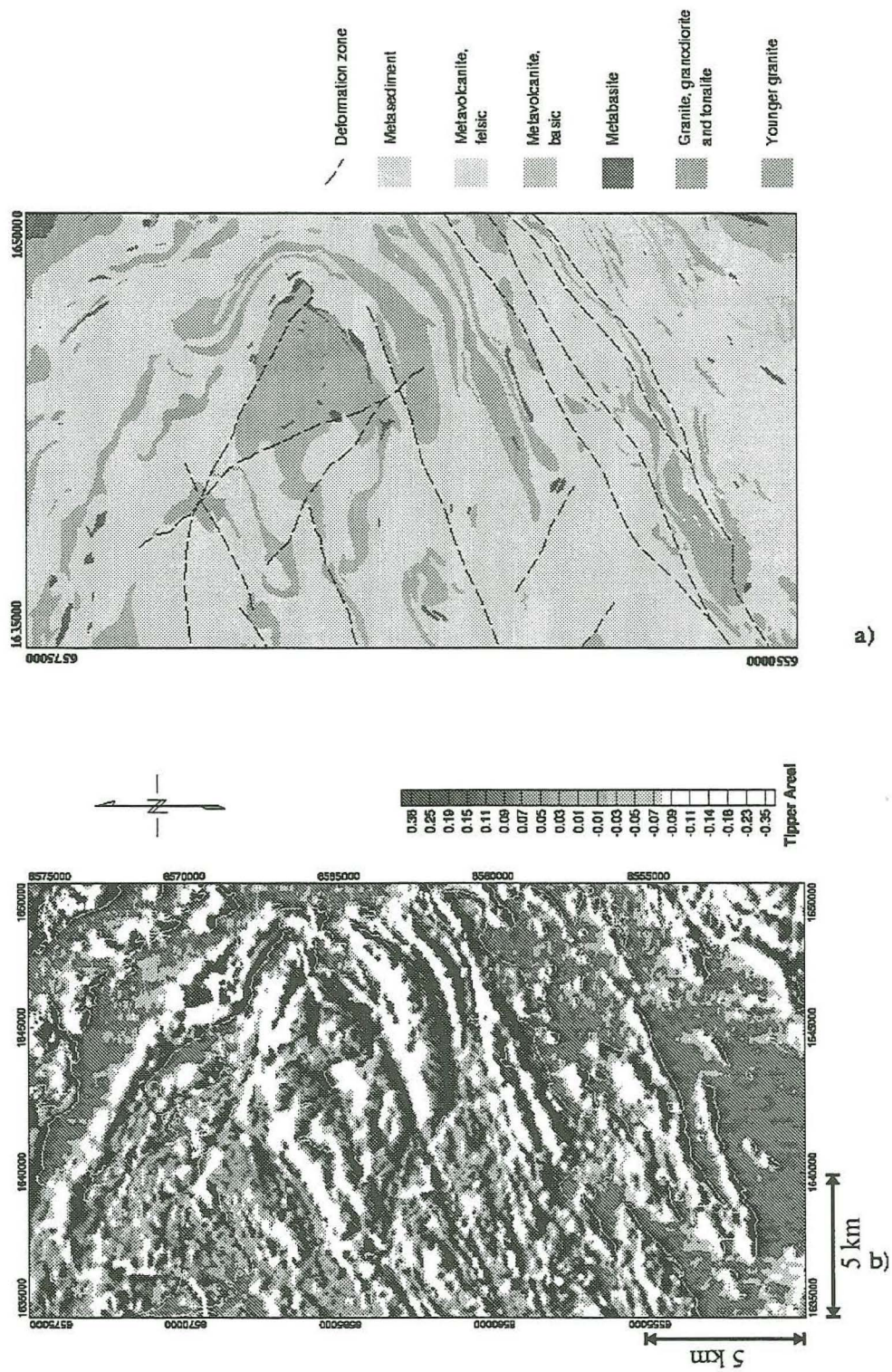
Figure 1: Simplified geological map (a) and example of magnetic transfer functions (b). Data are from SGU database, copyright *the Geological Survey of Sweden, 2000*.
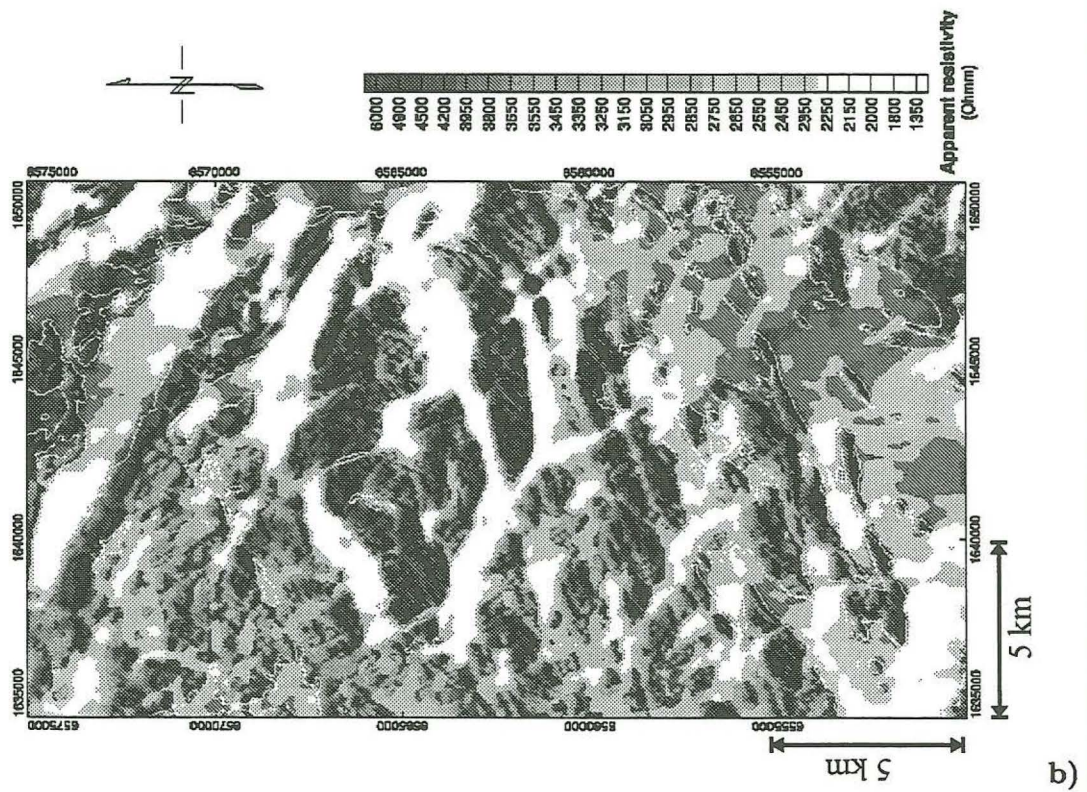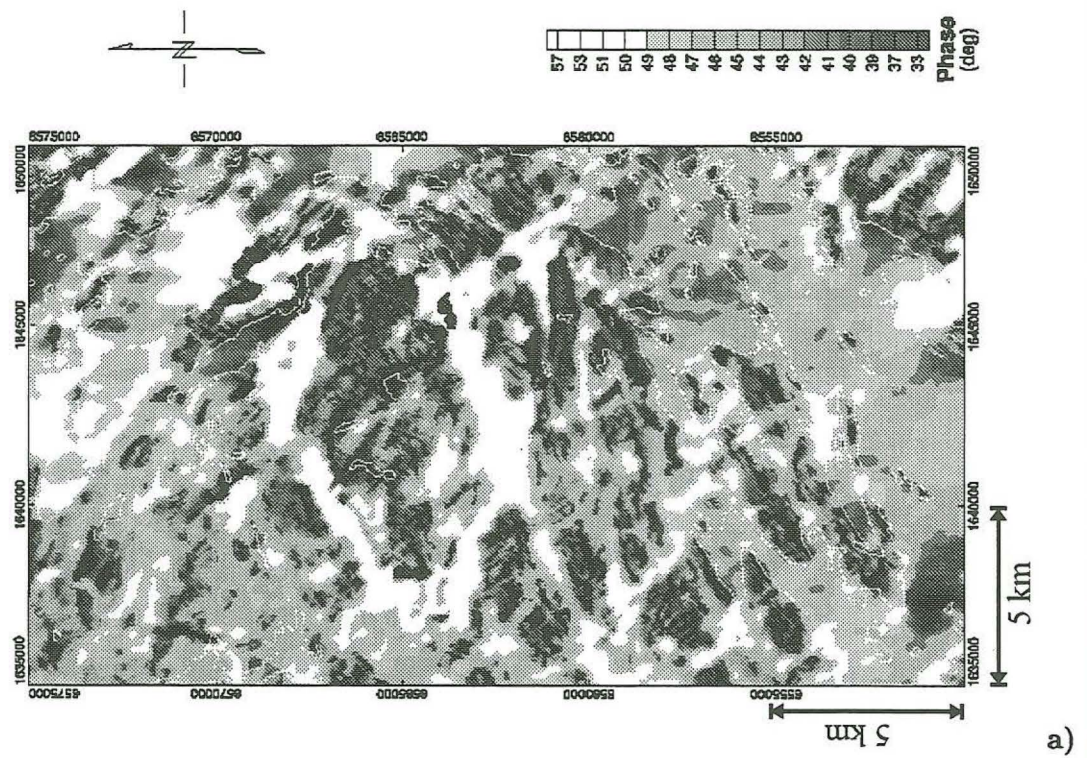
Figure 2: Results of the tipper transformation. See text for description. Data are from SGU database, copyright *the Geological Survey of Sweden, 2000.*

indicating deep conductors in form of highly mineralized metasediments and metavolcanics (Allen et al. [1996]). The massive granitoid blocks shown in the geological map are clearly made out as electrically high resistive structures. Here, the phase is lower than 45 degrees, indicating an increasing resistivity with depth. This coincides with a simplified depth sequence of a thin layer of conductive overburden and an underlaying, highly resistive (but weathered in the near surface) crystalline rock.

Fault zones are marked by low resistivities (if they are fluid-filled) and build a pattern of south-southeast and east-northeast striking features. Many details given in the geological map can be recovered from the map of apparent resistivities, and vice versa, but this will not be described further here.

The results presented above are very satisfactory and are easily interpreted. Improvements could be achieved by using two transmitters perpendicular to each other to enhance resolution of north-striking features and by using more frequencies to improve depth resolution.

Conclusion

First, the transformation of magnetic transfer functions into apparent resistivities and phases is a new representation of the data. Interpretation of magnetic transfer functions is rather difficult, because they indicate lateral changes of the earth's resistivity distribution. Information of the depth dependency of the structures is given in terms of the mutual sign relation between real and imaginary part of the transfer functions, e.g. its phases. Extracting this information cannot be obtained by visually analyzing the maps. The new representation in terms of apparent resistivity and phases clearly indicates lithological units and an idea about the depth profile by interpreting phases.

The derivation of apparent resistivities and phases is based on an iterative approach, exploiting the potential field character of the magnetic field in the air half-space and the properties of the electric field offered by the mode decomposition in TE- and TM-mode. Only a simple mathematical equipment is required to estimate the electric field of TE-mode besides a constant. This enables the processing of large data sets in a reasonable time. The unknown constant has to be known by other means, for instance by an impedance ground measurement. We favored to guess the medium electric field over the whole area by assuming a kind of medium structure. This turned out to be quite reasonable. In any case one should be aware, that the transformation does not yield apparent resistivities and phases one would actually estimate from magnetic *and* electric field measurements (impedance measurements). Therefore, a wrong level of amplitudes caused by a wrong guess of the medium electric field does not degrade the results.

Acknowledgments

References

Allen R. L., Lundstroem, I., Ripa, M., Simeonov, A., Christofferson, H., 1996. Facies Analysis of a 1.9 Ga, Continental Margin, Back-Arc, Felsic Caldera Province with Diverse Zn-Pb-Ag-(Cu-Au) Sulfide and Fe Oxide Deposits, Bergslagen Region, Sweden, *Economic Geology*, **91**,

979-1008

Gharibi, M., Pedersen, L. B., 2000: Transformation of VLF data into apparent resistivities and phases, *Geophysics*, **64**, 1393-1402

Pedersen, L. B., 1989. Relations between horizontal and vertical gradients of potential fields, *Geophysics*, **64**, 662-663.

Pedersen, L. B., Qian, W., Dynesius, L., and Zhang, O., 1994. An airborne tensor-VLF system: From concept to realization: *Geophys. Prosp.*, **42**, 863-883.

Vanyan, L. L., Varentsov, I. M., Golubev, N .G., Sokolova, E. Yu., 1998. Derivation of Simultaneous Geomagnetic Field components from Tipper Arrays, *Izvestiya - Physics of the Solid Earth*, **34**, 89-96

Vasseur, G. & Weidelt, P. 1977. Bimodal electromagnetic induction in non-uniform thin-sheets with an application to the northern Pyrenean anomly, *Geophys. J. R. astr. Soc.*, **51**, 669-690.

Weidelt, P., Lecture Notes. unpublished